RSC Advances

ROYAL SOCIETY OF CHEMISTRY

www.rsc.org/advances

RSC Advances

RSCPublishing

ARTICLE

Electrochemical and theoretical study of the inhibition effect of two synthesized thiosemicarbazide derivatives on carbon steel corrosion in hydrochloric acid solution

Cite this: DOI: 10.1039/x0xx00000x

Received ooth January 2012,
Accepted ooth January 2012

DOI: 10.1039/x0xx00000x

www.rsc.org/

Shirin Shahabi[a], Parviz Norouzi[*a,b], Mohammad Reza Ganjali[a,b]

In this work, two thiosemicarbazide derivatives, 2-Carbamothioyl-N-phenylhydrazine carboxamide (TSC1) and N-[(2-Carbamothioylhydrazino)carbonothioyl]benzamide (TSC2) are synthesized and used as carbon steel corrosion inhibitors in 1.0 M HCl. Weight loss measurements indicate that the studied compounds reduce the corrosion rate of carbon steel in acidic solution and the inhibition effect increase with the inhibitors concentration. It was also shown that the adsorption of TSC1 and TSC2 followed a Langmuir adsorption isotherm. Tafel polarization method reveals that the organic compounds act as mixed type corrosion inhibitors with predominantly anodic effect. Electrochemical Impedance Spectroscopic measurements show that the inhibitors form an adsorptive layer on the metallic surface and increase the polarization resistance of the corrosion reaction. Fast Fourier Transform Continuous Cyclic Voltammetry is used to continuously monitor the inhibitors adsorption behavior on the carbon steel surface. The results indicate that TSC2 can better inhibit the carbon steel corrosion rather than TSC1. Some of the inhibitors quantum chemical parameters are calculated with DFT method at B3LYP/6-31g(d,p) level of theory. Among calculated parameters, LUMO energy, energy gap between HOMO and LUMO and hardness could well describe the experimental observations.

1.Introduction

Metallic corrosion causes severe losses to both economy and safety. Therefore, many research efforts have been made to prevent or decrease the corrosion of metals in different mediums.[1-5] Hydrochloric acid (HCl) is an important inorganic acid that is used in many industries. For example, one of the main applications of HCl is its usage in the pickling baths to remove rust or scale from iron or steel before subsequent processing.[6,7] However, when HCl is in contact with metals, it starts to corrode the metallic surfaces. So, in spite of its benefits, it is necessary to find a way for lessening the corrosion rate when HCl is used. Carbon steel has been widely used in various industries and consequently has been subjected to acid corrosion in its different situations.[8-10] An economic and operative solution to the corrosion problem is the use of corrosion inhibitors. Inhibitors are chemicals that when added to the corrosive solution at small amounts, decrease the corrosion rate at noticeable extent.[10-14] Inhibitor molecules are adsorbed on the metallic surface resulting in formation a barrier between the surface and the corrosive medium. Generally, organic inhibitors are adsorbed on the metallic surface through their hetroatoms or π-orbitals. However, their effectiveness depends on the quality of adsorption and consequently their structural and electronic properties. In recent years, in parallel with hardware and software developments, many attempts have been done to relate the inhibition efficiency of inhibitors to their physicochemical and electronic properties, which obtained by theoretical calculations.[15-120] Quantum chemical calculations are used to calculate structural and electronic properties of molecules and materials. DFT is presently among most successful approaches to investigate the electronic structure of atoms, molecules, solids and even nuclei and classical fluids.[21-24]

The objective of this work is the investigation of inhibition effect of two thiosemicarbazide derivatives on carbon steel corrosion in 1.0 M HCl solution by weight loss measurements, Tafel polarization method, Electrochemical Impedance Spectroscopy (EIS), Fast Fourier Transform Continuous Cyclic Voltammetry (FFTCCV) and DFT calculations.

2 Experimental

2.1 Synthesize of inhibitors

Fig. 1 shows the molecular structures and IUPAC names of the inhibitors, TSC1 and TSC2, which is used as carbon steel corrosion inhibitors. A mixture of phenylisocyanate (1.0×10^{-2} mol), thiosemicarbazide (1.0×10^{-2} mol) and a catalytic amount of acetic acid was refluxed in 70 mL ethanol for 2 h to synthesize TSC1. Then the solvent was evaporated to 20 mL. After cooling to room temperature, the product was obtained as crystals. To synthesize TSC2, a mixture of ammoniumthiocyanate (2.0×10^{-3} mol) and HCl (2.0×10^{-3} mol) was warmed at about 50°C for 5 min. Then, thiosemicarbazide (2.0×10^{-3} mol) was added and stirred for 3 h at room temperature, and at the end poured into 15 mL of water. The obtained precipitation was separated by filtration and recrystallized from ethanol to afford the pure compounds.

The inhibitor compounds were characterized by ^{1}HNMR and ^{13}CNMR data the studied inhibitors are listed as below: For TSC1: ^{1}H NMR/DMSO/δ ppm: 10.7 (s, 1H), 9.72 (s, 2H), 9.02 (s, 1H), 8.16 (s, 1H), 7.44 (d, J = 7.5 Hz, 2H), 7.30 (t, J = 7.3 Hz, 2H), 7.11(t, J = 7.5 Hz IH). ^{13}C NMR/DMSO/d ppm: 182.8, 151.4, 133.2, 127.6, 120.4, 118.9. For TSC2: ^{1}H NMR/DMSO/δ ppm: 11.15 (s, 1H), 10.06 (s, 2H), 9.44 (s, 2H), 7.82 (d, *J* = 7.8 Hz, 2H), 7.61 (t, *J* = 7 Hz, 2H), 7.27 (t, *J* = 7.2Hz, 1H). ^{13}C NMR/DMSO/d ppm: 180.3, 175.5, 164.2, 137.2, 133.5, 126.5, 122.5.

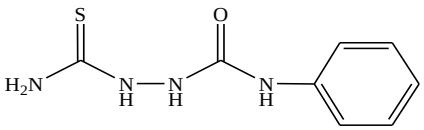

2-Carbamothioyl-N-phenylhydrazinecarboxamide (TSC1)

(a)

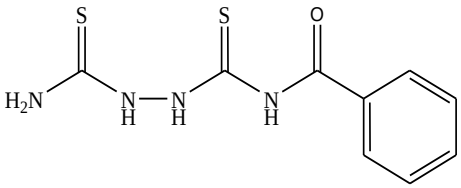

N-[(2-Carbamothioylhydrazino)carbonothioyl]benzamide (TSC2)

(b)

Fig. 1 Molecular structure of compounds TSC1 and TSC2 and their IUPAC names.

2.2 Carbon steel samples and solutions

A carbon steel sample containing (wt%) C 0.326 %, Si 0.235 %, Mn 0.742 %, P 0.016 %, Cr 0.073 %, Ni 0.0145 %, Al 0.022 %, S 0.017 %, Cu 0.129 %, V 0.001 % and the rest iron, was used to construct the working electrode. Before doing each run, the electrode surface was polished with different grades of emery papers (which ended with the 1200 grit), degreased in ultrasonic bath with ethanol and acetone and finally rinsed with distilled water. The aggressive solution of 1.0 M HCl was prepared by dilution of 36 % HCl from Merck with distilled water. In order to solve the solubility problems, the inhibitor solutions were prepared in 1.0 M HCl containing 5 % v/v DMSO. Obviously, this volume of DMSO was also added to the blank solution.

2.3 Weight loss experiments

The weight loss of the carbon steel strips of 5.0 cm ×2.5 cm ×0.2 cm in 1.0 M HCl in the absence and presence of various concentrations of the inhibitors are determined at 25 °C. Before doing each experiment, the carbon steel surface was abraded with emery papers (up to 1200 grit), then cleaned in ultrasonic bath with ethanol and acetone, and finally washed with distilled water. After weighing accurately, the specimens were immersed in 100 mL corrosive solution for 1 h. Then, the specimens were taken out, cleaned, dried and reweighed. The experiments were done in triplicate and the average value of the weight loss was used.

2.4 Electrochemical measurements

A three-electrode set-up was composed of a Pt counter electrode (CE), an Ag/AgCl reference electrode (RE), and carbon steel working electrode (WE) was used for electrochemical measurements. Polarization measurements were done by an AUTOLAB model PGSTAT30, which was connected to a personal computer to record and store the electrochemical data. Anodic and cathodic polarization curves were recorded by sweeping the potential from a more positive potential than Eocp to a more negative potential at a scan rate of 1.0 mV/s. The polarization data was analyzed using GPES software. The inhibition efficiencies (IE %) was calculated according the Eq. (1).[25]

$$IE\% = \frac{I_{corr,uninhibit} - I_{corr,inhibit}}{I_{corr,\ uninhibit}} \times 100 \quad (1)$$

where the $I_{corr,uninhibit}$ and $I_{corr,inhibit}$ are the corrosion current density without and with inhibitors, respectively.

The EIS measurements were started at E_{ocp} using an AC signal (5 mV peak to peak) at the frequency range of 5.5×10^{-2} Hz to 1.0×10^{5} Hz. EIS data were analyzed with FRA software. Polarization resistance (R_p) and constant phase element (CPE) were obtained from Nyquist plots. The IE % values were calculated from the R_p values according Eq. (2).[26]

$$IE\% = \frac{R_{p,inhibit} - R_{p,uninhibit}}{R_{p,inhibit}} \times 100 \quad (2)$$

where $R_{p,inhibit}$ and $R_{p,uninhibit}$ are the polarization resistance of inhibited and uninhibited solutions, respectively.

To apply FFTCCV runs, a custom-made potentiostat was connected to a PC equipped with a data acquisition board (PCL-818HG, Advantech. Co.). The potential was repeatedly swept between an initial and a final potential, which are more negative and more positive than corrosion potential (E_{corr}). As a result, numerous cyclic voltammograms were recorded repeatedly. The sweep rate was equal to 1.0 V/s, which was the lowest sweep rate that could be accessible for the instrument. The potential waveform used in this technique is shown in Fig 2.

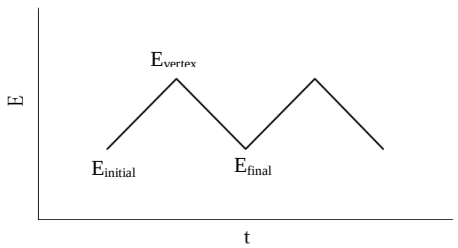

Fig. 2 Diagram of the applied potential waveform.

2.5 SEM experiments

A Hitachi 460 SEM was used to observe the surface morphology of carbon steel samples before and after 24 h immersion in 1.0 M HCl solution in the absence and presence of inhibitors.

2.6 Quantum chemical calculations

Geometry optimizations were done using standard Gaussian-03 software package[27] with B3LYP functional and a 6-31G(d,p) basis set.[28, 29] DFT methods are considered to be a standard method for modeling many chemical processes.[22,30] BLYP is a popular functional which derived from the combination of Becke[31] for the exchange part and Lee, Yang and Parr[32] for the correlation part. The more broadly used, B3LYP, is a hybrid functional in which the exchange energy, from Becke's three-parameter functional (B3), is combined with the exact energy from Hartree-Fock theory.

The calculated quantum chemical parameters are energy of the Highest Occupied Molecular Orbital (E_{HOMO}), energy of the Lowest Unoccupied Molecular Orbital (E_{LUMO}), energy gap ($\Delta E = E_{LUMO} - E_{HOMO}$), dipole moment (D), electron affinity (A) and hardness (η).

3 Results and discussion

3.1 Weight loss measurements

The values of the inhibition efficiencies obtained from the weight loss measurements are presented in Table 1 for different concentrations of the inhibitors. The corrosion rate (CR) is calculated from the following equation:[33]

$$CR = \frac{m_1 - m_2}{S.t} \quad (3)$$

where m_1 is the mass of the carbon steel sheet before immersion (mg), m_2 is the mass of the mass of the carbon steel sheet after immersion (mg), S is the total area of the carbon steel sheet (cm^2), t is the corrosion time (h) and CR is the corrosion rate (mg cm^{-2} h^{-1}). The surface coverage (θ) and %IE are calculated using the following equations:[33]

$$\theta = \frac{CR_{uninhinit} - CR_{inhibit}}{CR_{uninhibit}} \quad (4)$$

$$IE\% = \frac{CR_{uninhinit} - CR_{inhibit}}{CR_{uninhibit}} \times 100 \quad (5)$$

where $CR_{uninhibit}$ and $CR_{inhibit}$ are the values of carbon steel corrosion rates in uninhibited and inhibited solutions, respectively. From the Table, it is obvious that with increasing the inhibitors concentration, the corrosion rate decreases and conversely, the inhibition efficiency increases. The data in Table 1 demonstrates that the maximum inhibition efficiency was obtained for the solution containing 1.0×10^{-3} M TSC2. It is concluded that for carbon steel corrosion inhibition in 1.0 M HCl, TSC2 acts more efficiently than TSC1.

Table 1 Weight loss results of carbon steel corrosion in 1.0 M HCl solution in the absence and presence of various concentrations of the inhibitors TSC1 and TSC2.

Inhibitor	C_{inh} (M)	CR (mg cm^{-2} h^{-1})	θ	IE (%)
Blank	–	5.31		-
TSC1	1.0×10^{-4}	0.92	0.83	82.7
	5.0×10^{-4}	0.81	0.85	84.7
	8.0×10^{-4}	0.73	0.86	86.3
	1.0×10^{-3}	0.53	0.90	90.0
TSC2	1.0×10^{-4}	0.60	0.89	88.7
	5.0×10^{-4}	0.47	0.91	91.1
	8.0×10^{-4}	0.43	0.92	91.9
	1.0×10^{-3}	0.39	0.93	92.7

3.2 Polarization measurements

Fig. 3a and b show Tafel polarization plots of carbon steel in 1.0 M HCl without and with different concentrations of thiosemicarbazide compounds. Fig. 3 represents that both anodic and cathodic current densities decreased in the presence of the investigated compounds. This decrease is more pronounced with the growth in inhibitors concentration. This observation demonstrates that the inhibitors are adsorbed on the carbon steel surface. Consequently, this adsorption reduces both anodic dissolution of iron at anodic sites and cathodic evolution of hydrogen at cathodic sites. As the inhibitors concentration rises, the extent of adsorption increases, leading to increased inhibition efficiency. The obtained corrosion parameters including corrosion current density (I_{corr}), corrosion potential (E_{corr}) and electrochemical kinetic parameters i.e. anodic and cathodic Tafel slopes (b_a and b_c) for different concentrations of inhibitors are listed in Table 2.

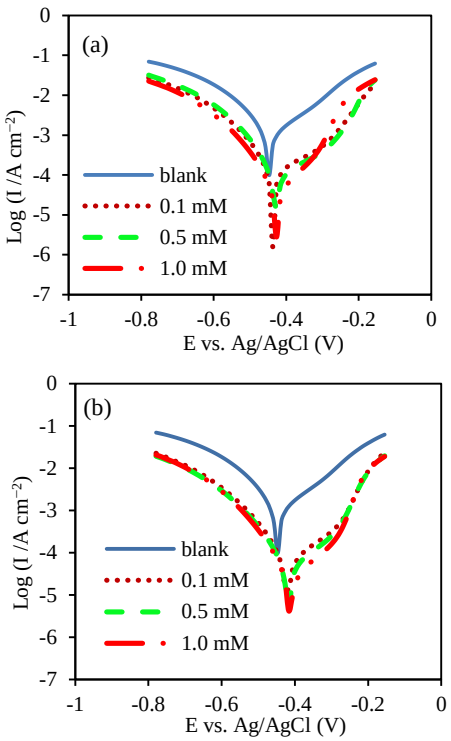

Fig. 3 Polarization curves of carbon steel electrode in 1.0 M HCl solution without and with different concentrations of (a) inhibitor TSC1 and (b) inhibitor TSC2.

Table 2 shows that the maximum and minimum inhibition efficiencies were respectively obtained for the solutions containing 1.0 mM of compounds TSC2 and TSC1, which is in agreement with the weight loss results. The values of Tafel slopes represent alteration in both anodic and cathodic slopes, showing the effect of the inhibitors on both anodic and cathodic processes. From Table 2, the maximum shift in Tafel curves is equal to 40.0 mV, which is related to the presence of 1.0 mM of TSC2 in HCl solution. These observations approve that all investigated compounds are mixed-type or adsorptive inhibitors with primarily anodic inhibition effect.[34-37]

Table 2 Polarization parameters for carbon steel in 1.0 M HCl solution in the absence and presence of various concentrations of the inhibitors TSC1 and TSC2.

Inhibitor	C_{inh} (M)	$-E_{corr}$ (mV)	i_{corr} ($\mu A\ cm^{-2}$)	$-b_c$ ($mV\ dec^{-1}$)	b_a ($mV\ dec^{-1}$)	IE (%)
Blank	–	455	461.30	137	111	-
TSC1	1.0×10^{-4}	437	82.58	141	115	82.1
	5.0×10^{-4}	427	73.60	133	118	84.0
	1.0×10^{-3}	428	47.14	141	121	89.8
TSC2	1.0×10^{-4}	421	51.04	142	131	88.9
	5.0×10^{-4}	416	41.12	141	138	91.1
	1.0×10^{-3}	415	35.20	150	137	92.4

3.3 EIS measurements

Nyquist plots of carbon steel electrode in 1.0 M HCl in the absence and presence of different concentrations of the inhibitors TSC1 and TSC2 are represented in Fig. 4 a and b, respectively. It is obvious from Fig. 4 that the impedance diagrams of investigated inhibitors simply yield depressed semicircles. As seen in the figure, the diameter of the semicircles increases with increasing the inhibitors concentration. The simple -R(CR)- model could well describe such situation at the metal/solution interface. The capacitor element is referred to double layer between the charged metal surface and the solution. Such depressed semicircle shape in the Nyquist plots are indication of non-ideality in capacitive behavior . this non-ideality is attributed to frequency dispersion resulting from different physical phenomena such as inhomogeneities, impurities, grain boundaries and also mass transport resistance.[38-40] So, in the equivalent circuit, which was developed to fit the experimental data, a capacitive element (ideal capacitor) is replaced by a constant phase element (CPE). Fig. 5 shows the corresponding equivalent circuit, where R_p is the polarization resistance, R_s is the solution resistance and as mentioned earlier, CPE represents a constant phase element. Such equivalent circuit has been previously used to model the metal/acid interface.[44-45] A CPE has two parameters: Q and n. The impedance of this element is given by the following equation.[44]

$$Z_{CPE}=Q^{-1}(j\omega)^{-n} \quad (6)$$

where Q is the magnitude of the CPE, j is the imaginary number, ω is the sine wave angular frequency (ω= 2πf, the frequency in Hz) and $-1\leq n\leq 1$ is the phase shift, which gives details about the degree of surface inhomogeneity. When n= 0, the CPE converts to a pure resistor. If n= +1, the CPE becomes a pure capacitor where CPE characterizes C_{dl}, and if n= −1, the CPE becomes an inductor.[43,44] In fact, when n is close to 1, the CPE is similar to a capacitor, but the phase angle is not 90°. It is constant and somewhat less than 90° at all frequencies.

The IE % values were calculated using R_p values by previously mentioned equation (Eq. 2). The polarization resistance (R_p) must be corresponding to the resistance between the metal and outer Helmholtz plane (OHP) and could be simply calculated from the difference in impedance at lower and higher frequencies.[46-48] Calculated EIS parameters, namely Q, R_p and n are presented in Table 3. These data revealed that after the addition of inhibitors R_p values increased and Q values decreased. It can be concluded that the adsorption of inhibitor molecules at the steel surface causes a reduction in the local dielectric constant and growth in the thickness of electrical double layer, leading to decrease in Q values and increase in R_p values. In fact, replacement of water molecules and other ions originally adsorbed on the surface (with high dielectric constant) with organic inhibitor molecules (with low dielectric constants) creates these changes in electrical characteristics of the carbon steel/solution interface. Besides, the values of phase shift (n) in Table 3 are in the range between 0.86 and 0.91. In view of that, there is not any substantial change in the value of n in the absence and in the presence of inhibitors under investigation, indicating that the charge transfer process controls the dissolution mechanism of carbon steel in 1.0 M HCl solution in the absence and presence of studied inhibitors. Like weight loss and polarization results, EIS measurements point out that the order of IE % for the inhibitors is TSC2>TSC1.

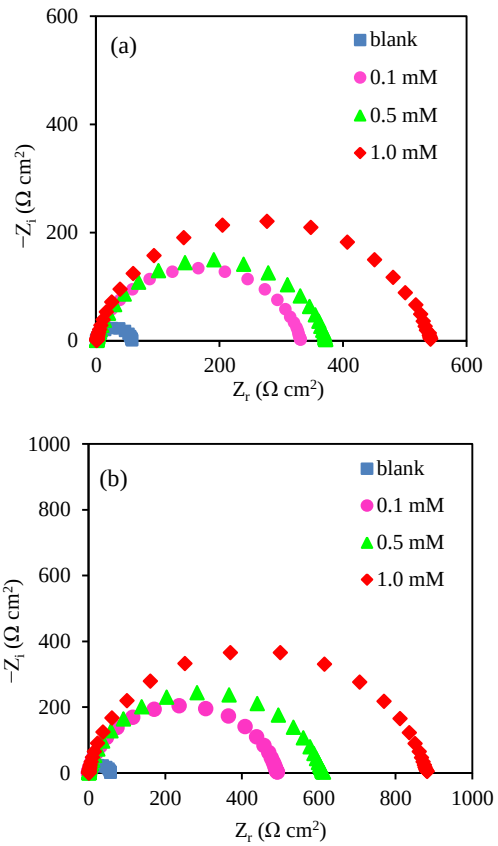

Fig. 4 Nyquist Impedance plots of carbon steel electrode obtained in 1.0 M HCl solution in the presence of various concentrations of (a) TSC1, (b) TSC2.

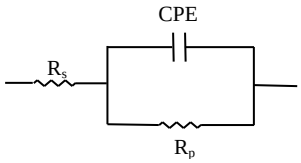

Fig. 5 Electrical equivalent circuit used for demonstrating carbon steel/solution interface.

Table 3 Electrochemical impedance parameters for carbon steel in 1.0 M HCl solution in the absence and presence of various concentrations of the inhibitors TSC1 and TSC2.

Inhibitor	C_{inh} (M)	R_p (Ω cm^2)	n	CPE ($\mu\Omega^{-1}$ s^n cm^{-2})	IE (%)
blank	-	57.8	0.86	305.7	-
TSC1	1.0×10^{-4}	334.2	0.86	35.2	82.7
	5.0×10^{-4}	378.8	0.86	30.1	84.7
	1.0×10^{-3}	538.8	0.88	26.5	89.3
TSC2	1.0×10^{-4}	484.7	0.89	29.5	88.1
	5.0×10^{-4}	596.9	0.88	18.7	90.3
	1.0×10^{-3}	861.1	0.91	17.4	93.3

3.4 SEM studies

The surface morphology of the carbon steel samples was examined by SEM after the sample was immersed in 1.0 M HCl solution in the absence and presence of the inhibitors. Fig. 6a shows the morphology of freshly polished carbon steel surface. It could be seen that there are some imperfections and mechanical faults on the polished surface. The carbon steel surface, which has been immersed in 1.0 M HCl solution in the absence of inhibitors, is shown in Fig. 6b. The roughened corroded surface and presence of considerable amounts of corrosion products are indications for acidic corrosion of carbon steel surface in noticeable extent. Fig. 6c and d represent the SEM images of carbon steel surface after immersion in acidic solution containing 1.0×10^{-3} M of the inhibitors TSC1 and TSC2, respectively. These images clearly show the more protected carbon steel surface, which results from the adsorption of inhibitors on the steel surface and reduction of the corrosion rate. This protection is more obvious for the solution containing the inhibitor TSC2

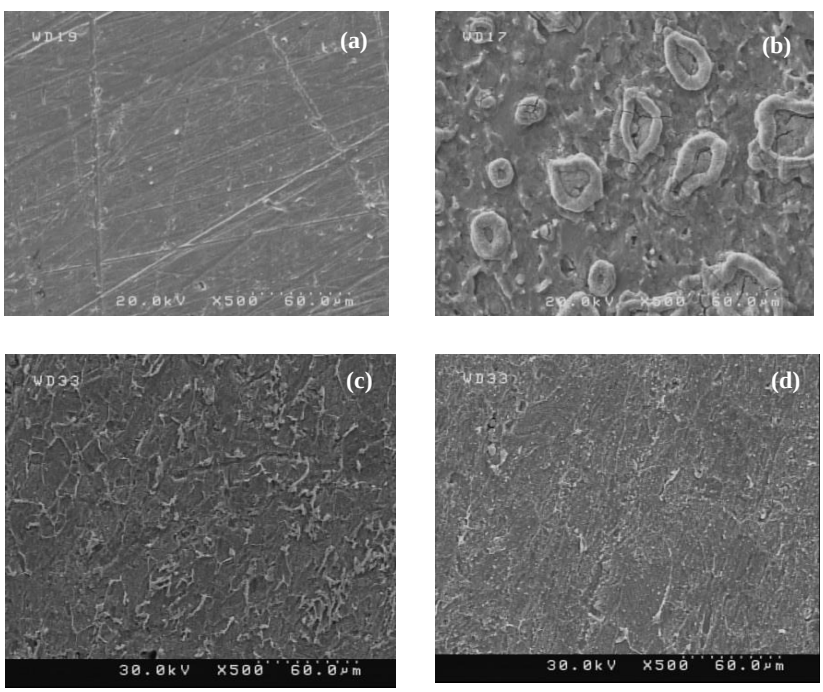

Fig. 6 SEM images of carbon steel for freshly polished surface (a) and after 24 h immersion in 1.0 M HCl solution without inhibitors (b) and with 1.0×10^{-3} M of TSC1 (c) and TSC2 (d).

3.5 FFTCCV measurements

FFTCCV was used to continuously monitor the changes of current passed through th electrode during the immersion time. These changes are related to the adsorption behavior of the inhibitors on the electrode surface. In this technique, the potential waveform was continuously applied during the experiment and variation of the charge under peak was monitored. As a result, a large number of CV curves were recorded and displayed in real time, which could be used to study the changes in carbon steel surface and the adsorption process.

In order to extract the information about the adsorption processes and the changes in the double layer at the electrode surface[49], the background current in voltammetric measurements must be removed from the recorded CV curves. The following equation was used for the background subtraction in the software program.[50-52]

$$\Delta i(s, E) = i(s, E) - i(s_r, E) \quad (7)$$

where s is the sweep number, i(s, E) represents the CV curve recorded during the s-th sweep and $i(s_r, E)$ is the reference CV curve. The reference CV curve was obtained by averaging three CV curves recorded at the beginning of each experiment.

In practice, CV curves are recorded numerically by sampling current in equal time intervals. As a result, we will have differential cyclic voltammograms, which have been obtained using eq. 3. Fig. 7a shows the differential CV curves of the carbon steel electrode in HCl solution without any inhibitors. Fig. 7b and c show differential CV curves of the electrode in HCl solution in the presence of 5.0×10^{-4} M TSC1 and TSC2, respectively. For each experiment the electrode was immersed for 70 minutes in the acidic solution. As expected, the net current change for the blank solution (up to 8.0 mA) is larger than the electrode in the inhibitor containing solutions. The net change of corrosion current for the electrode in the solution containing inhibitors TSC1 and TSC2 are respectively around 4.3 mA and 3.5 mA, which obtained from the maximum of the differential CV curves. These results approve that both of the investigated thiosemicarbazide derivatives inhibit the corrosion of carbon steel in HCl solution, and so reduce the change of current which is due to the corrosion process in real time. Results also confirm the weight loss, Tafel, EIS and SEM results which indicate better performance of TSC2 rather than TSC1.

Moreover, Overlay differential CV curves in Fig. 7b and c show that at the start of the experiment, the slope of the curves maximums versus time is relatively large and at the end, it progressively becomes smaller until reaches to unchanging values. The time for achievement of such state for TSC1 and TSC2 is about 3500 s and 2800 s, respectively. It could be concluded that the adsorption of inhibitor TSC2 took place considerably faster than the inhibitor TSC1. Therefore, at a shorter time, TSC2 reaches to its maximum surface coverage.

For giving further information about the adsorption behavior of studied inhibitors, the integration of current at the specified potential range was performed in real time. The following equation is theoretical approach for calculation of the charge under a cyclic voltammogram at the potential range E_1 to E_2:

$$Q_t = \frac{1}{\nu}\int_{E_1}^{E_2} I_{(E)}\, dE \quad (8)$$

where ν is the scan rate.

As previously mentioned, CV curves are recorded numerically by sampling current in equal time intervals. Therefore, we used the following equation to integrate the current over the potential range, E_1 to E_2, and calculate the total charge ΔQ:[53-55]

$$\Delta Q(s,t) = \Delta t\left(\sum_{E=E_1}^{E=E_2} I(s,E) - \sum_{E=E_1}^{E=E_2} i(s_r,E)\right) \quad (9)$$

where s is the sweep number, t is the time period between subsequent sweeps, Δt is the time difference between two subsequent points on the CV curves, i (s, E) represents the CV curve recorded during the s-th sweep and $I(s_r, E)$ is the reference CV curve.

Fig. 8 represents the plot of ΔQ as a function of time for carbon steel electrode during 70 minutes immersion 1.0 M HCl in the absence and presence of 5.0×10^{-4} M TSC1 and TSC2. The slope of this plot in the solution containing inhibitors is considerably more than the slope in the solution without any inhibitors. This reduction seen in the slope demonstrates that in the presence of the inhibitors, the corrosion rate of carbon steel decays significantly. The results, also, indicate that in the presence of inhibitor TSC2, this decay is in its maximum value.

3.6 Adsorption isotherm

In order to gain more information about the mode of the studied inhibitors adsorption on the carbon steel surface, the data from weight loss measurements have been used to explain the best isotherm that defines the adsorption process. In order to find the best adsorption isotherm, which describe the adsorption of TSC1 and TSC2 on the carbon steel surface, several isotherms Langmuir, Temkin and Frumkin, have been tested. However, the best fit is obtained with the Langmuir isotherm, which is shown in Fig. 9. The Langmuir isotherm is defined according to Eq. 10:[56,57]

$$\frac{C_{inh}}{\theta} = \frac{1}{k_{ads}} + C_{inh} \quad (10)$$

where θ denotes the surface coverage, C_{inh} is the inhibitor concentration and K_{ads} is the adsorption equilibrium constant. The value of K_{ads} process is related to the standard free energy of adsorption, ΔG_{ads}, and equated as below:[56,57]

$$\Delta G_{ads} = -RT \ln 55.5 k_{ads} \quad (11)$$

In this equation, R is the gas constant (8.314 J/K mol), T is the absolute temperature (K) and 55.5 is the concentration of water in the solution (M).[58] The thermodynamics parameters derived from Langmuir adsorption isotherms for the studied inhibitors are given in Table 4. The negative values of ΔG_{ads} demonstrate a spontaneous adsorption process.[59,60] Generally, the energy values of −20 kJ mol^{-1} or less negative are related with an electrostatic interaction between charged molecules and charged metal surface (physisorption); the values of −40 kJ mol^{-1} or more negative involve charge sharing or transfer between the inhibitor molecules to the metal surface to form a coordinate bond (chemisorption).[58,61] The values of ΔG_{ads} between −40 kJ mol^{-1} and −20 kJ mol^{-1} demonstrate mixed type adsorption (both chemical and physical interactions). As shown in Table 4, the values of ΔG_{ads} for TSC1 and TSC2 are −36.6 kJ mol^{-1} and −39.1 kJ mol^{-1}, respectively. These values propose that the adsorption of these compounds involves two types of interaction, chemisorption and physisorption. However, the ΔG_{ads} values in this study, are more close to −40 kJ mol^{-1} demonstrating that the adsorption of TSC1 and TSC2 occurs predominantly by chemisorption.[39,61]

3.7 Molecular geometries and molecular orbital distribution

The optimized geometries of the molecules under investigation are presented in Fig. 10. These configurations are obtained by Gaussian03 package using DFT method at B3LYP/6-31G(d,p) level of theory, based on the absence of imaginary frequencies.

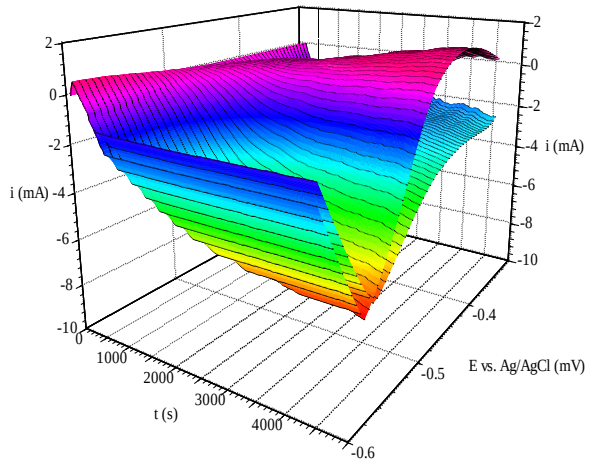

(a)

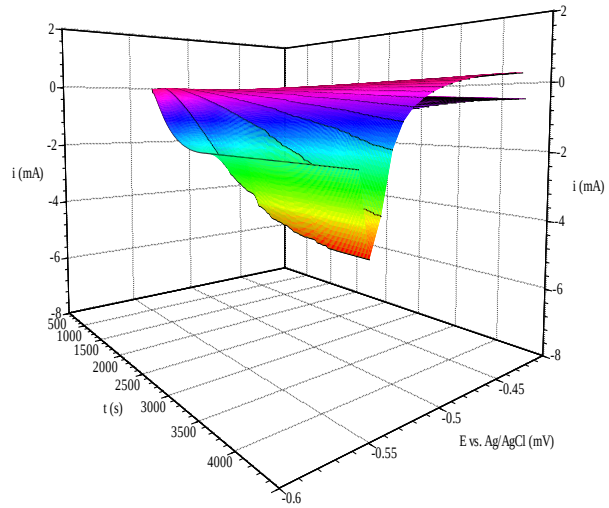

(b)

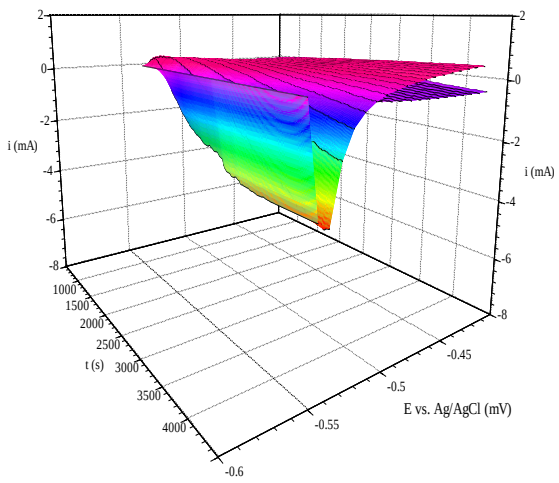

(c)

Fig. 7 Differential Continuous Cyclic Voltammogram of carbon steel electrode recorded during 70 minutes immersion in 1.0 M HCl solution without (a) and with 5.0×10^{-4} M of compound TSC1 (b) compound TSC2 (c).

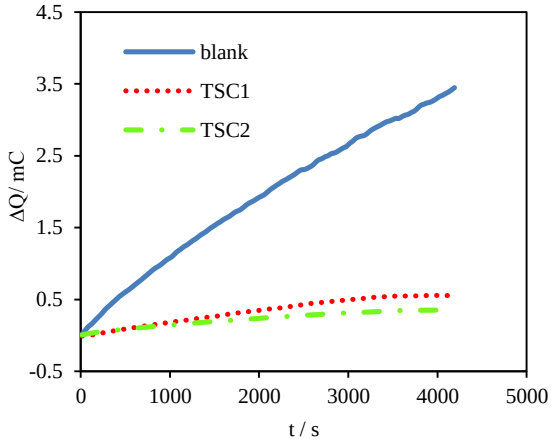

Fig. 8 Plot of total charge loaded by the steel electrode (ΔQ) vs. time in the blank solution and the solution containing 5.0×10^{-4} M of TSC1 and TSC2.

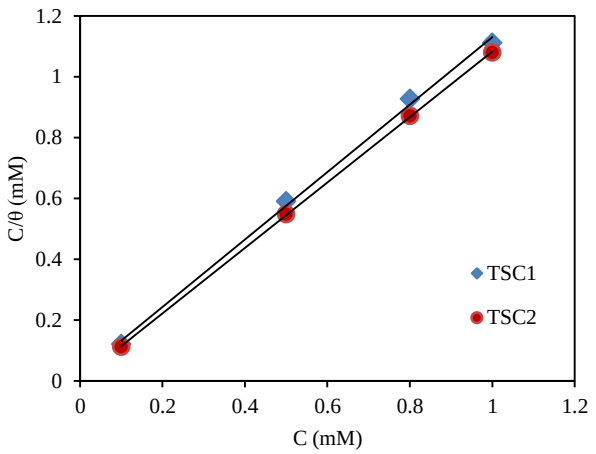

Fig. 9 Langmuir adsorption isotherm model for TSC1 and TSC2 on carbon steel surface.

Table 4 Thermodynamic parameters for the adsorption of TSC1 and TSC2 in 1.0 M HCl on thecarbon steel surfaceat 25 °C.

Inhibitor	R^2	K_{ads} (M^{-1})	ΔG_{ads} (kJ mol^{-1})
TSC1	0.998	46220.9	−36.6
TSC2	0.999	130679.5	−39.1

It could be seen that the inhibitor molecules are not fully planar, which may affect their inhibition efficiencies in comparison with similar structures with planar geometries. However, the planarity is just one of the factors affecting the inhibition performance of the molecules. Many other factors should be considered to evaluate the inhibitors effectiveness. It was shown that the effectiveness of an inhibitor depends on its electronic structure, in addition to its spatial molecular structure.

Consistent with Frontier Molecular Orbital (FMO) theory, developed by Kenichi Fukui[62], the frontier orbitals (HOMO and LUMO) of chemical species play a major role in describing its reactivity. Chemical reactions could be explained by interactions

between HOMO and LUMO on one or more molecules. FMO theory uses these foundational ideas to describe the structure and reactivity of molecules. In corrosion inhibition studies, FMO theory is useful in guessing the adsorption centers of the inhibitor that are responsible for the interaction with metal surface.[16,18] The HOMO and LUMO density distribution of the studied molecules are shown in Fig. 10. For these inhibitors, the NH_2 group at one end of the molecule has minimum or no density of the frontier molecular orbital distributions. Other parts of the molecules have contributions from the HOMO and LUMO populations. We should consider that the center of adsorption depends not only on the presence of HOMO and LUMO density on the special group, which is oriented toward the steel surface, but also on the approachability of the interaction site, the partial charge and the local reactivity of the atom or group. In order to find a logical explanation for the relative inhibition effect of the studied thiosemicarbazide derivatives, we need to consider the value of quantum chemical parameters in parallel with the spatial and electronic structure of the studied inhibitors. Table 5 shows some quantum chemical parameters of the studied inhibitors, which calculated with DFT method at B3LYP/6-31g(d,p) level of theory and some related equations.

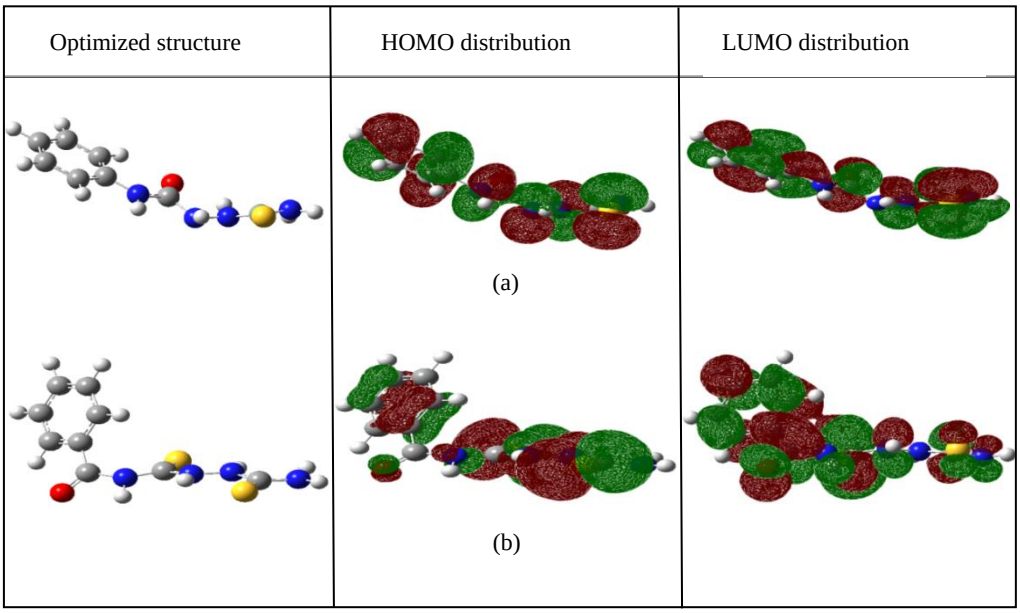

Fig. 10 Optimized structure, HOMO, and LUMO distribution of (a) TSC1 and (b) TSC2, calculated using DFT method at B3LYP/6-31G(d,p) level of theory.

Table 5 Some quantum chemical parameters for the studied inhibitors calculated using B3LYP/6-31G(d,p).

Inhibitor	E_{HOMO} (eV)	E_{LUMO} (eV)	ΔE (eV)	D (Debye)	A (eV)	η (eV)
TSC1	−5.90	−0.50	5.41	1.65	0.50	2.70
TSC2	−6.21	−1.75	4.46	4.23	1.75	2.23

E_{HOMO} is related to the electron donating ability of the molecule. A molecule with higher value of E_{HOMO} is more capable of giving electrons to an acceptor having appropriate vacant molecular orbitals. On the other hand, E_{LUMO} is related to the electron accepting ability of the molecule. Alternatively, the lower the value of E_{LUMO} indicates that it is more probable to receive electrons from an applicable donnor.[63,64] Based on experimental results, the order of inhibition efficiency for the studied inhibitors is TSC2>TSC1. From Table 5, the values of E_{HOMO} for the compounds TSC1 and TSC2 are −5.90 eV and −6.21 eV, respectively. If we consider that the investigated inhibitors just donate electrons to the Fe atoms at steel surface, we will consequently expect that the molecule with highest value of E_{HOMO} is the most effective inhibitor. However, experimental results do not confirm this assumption. It could be concluded that some other factors affect obtained experimental results. In previous works, it was found that the inhibitors that can accept electrons from metallic surface along with donate electrons to the surface would be better inhibitors.[42,65] As mentioned above, the value of E_{LUMO} is a good indicator for the electron accepting ability of a molecule. The values of E_{LUMO} for TSC1 and TSC2 are −0.50 eV and −1.75 eV, successively. According to the calculated values of E_{LUMO} and experimental findings, the reduction in E_{LUMO} values leads to increase in inhibition effect of the inhibitors. So, the values of E_{LUMO} could well describe the experimental results. The next parameter, $\Delta E = E_{LUMO} - E_{HOMO}$, is an important parameter to estimate the reactivity of a molecule. As ΔE decreases, the reactivity of the molecule increases, leading to an increase in adsorption of inhibitor molecules on the metallic surface and consequently an increase in the IE %. Table 5 shows that the value of ΔE for TSC2 is lower than TSC1 (4.46 eV < 5.41 eV), which is in good agreement with the experimental results. The next calculated quantum chemical parameter is dipole moment (D). Some authors state that %IE increases with increasing the value of the dipole moment. However, in some cases no significant relationship has been found between the

dipole moment values and the IE %.[66,67] In our study, increasing the dipole moment of the molecules leads to increase their inhibition efficiency as a result of increasing the intermolecular forces. In order to find proper quantum parameters to describe and predict the experimental results, we calculated some parameters using the parameters, which computed directly with DFT method. Electron affinity (A) is the change in energy of an atom or molecule (in the gaseous phase) when an electron is added to the atom or molecule to form a negative ion. The electron affinity is directly related to the energy of the LUMO:[68]

$$A = -E_{LUMO} \quad (12)$$

Table 5 shows that there is a good association between IE % and electron affinity, as well as E_{LUMO}. As the electron affinity value increases, the affinity of inhibitor to accept electrons from the metal surface into antibonding orbitals of inhibitor increases. As a result, the inhibition efficiency increases showing more protection for the metal surface.

Hardness of a compound is defined as the resistance against the deformation or polarization of the electron cloud under small perturbation. According to Pearson, the absolute hardness (g) of a chemical system is given by:[69]

$$\eta = \frac{(I-A)}{2} \quad (13)$$

In other words, a hard molecule has a large energy gap, and a soft molecule has a small energy gap. A high value of the absolute hardness is an indication of high stability and low reactivity. So, a molecule with low value of hardness would be adsorbed more easily than a molecule having high energy gap. In Table 5, the order of η for the studied inhibitors is TSC1> TSC2. Consequently, the order of reactivity would be TSC2> TSC1, which results in the higher IE% value for TSC2.

Conclusions

1) The investigated thiosemicarbazide derivatives (TSC1 and TSC2) inhibit the corrosion of carbon steel in 1.0 M HCl and their inhibition efficiency follows the order: TSC2 > TSC1.
2) The inhibitors are mixed type and adsorbed on the steel surface to block its active sites. This adsorption extends the double layer distance leading to a decrease in the double layer capacitance.
3) FFTCCV experiments show that the inhibitor TSC2 reaches to its maximum surface coverage at a shorter time than the inhibitor TSC1, indicating that the rate of adsorption of TSC2 is faster than adsorption of TSC1.
4) The adsorption of TSC1 and TSC2 molecules on the carbon surface in 1 M HCl solution obeyed Langmuir adsorption isotherm.
4) The experimental results are in good association with the parameters ELUMO, ΔE, dipole moment and hardness.

Acknowledgements

The authors express their appreciation to the University of Tehran Research Council for financial support of this work.

Notes and references

*Corresponding author. E-mail address: norouzi@khayam.ut.ac.ir.
[a] Center of Excellence in Electrochemistry, Faculty of Chemistry, University of Tehran, Tehran, Iran.
[b] Biosensor Research Center, Endocrinology & Metabolism Molecular-Cellular Sciences Institute, Tehran University of Medical Sciences, Tehran, Iran.

1 G. I. Ostapenko, P. A. Gloukhov and A. S. Bunev, *Corros. Sci.*, 2014, **82**, 265.
2 E. Ghali, V. S. Sastri and M. Elboujdaini, in *Corrosion Prevention and Protection: Practical Solutions*, John Wiley & Sons Ltd, Chichester, England, 2007.
3 R. Yıldız, A. Döner, T. Doğan and I. Dehri, *Corros. Sci*., 2014, **82**, 125.
4 A. O. Yüce, B. D. Mert, G. Kardaş and B. Yazıcı, *Corros. Sci*., 2014, **83**, 310.
5 D. Song, A. Ma, W. Sun, J. Jiang, J. Jiang, D. Yang and G. Guo, *Corros. Sci.* 2014, **82**, 437.
6 *Chemicals Economics Handbook*, SRI International, 2001.
7 N. N. Greenwood and A. Earnshaw in *Chemistry of the Elements*, Butterworth-Heinemann, 2nd edn., 1997.
8 J. Ochshorn, in *Steel in 20th Century Architecture: Encyclopedia of Twentieth Century Architecture*, 2002, Retrieved 2010.
9 P. A. Schweitzer, in *Fundamentals of metallic corrosion: atmospheric and media corrosion of metals*, CRC Press, Taylor & Francis Group, 2nd edn., 2007.
10 M. Lagrenée, B. Mernari, M. Bouanis, M. Traisnel and F. Bentiss, *Corros. Sci.* 2002, **44**, 573.
11 J. R. Davis in *Corrosion: understanding the basics*, Davis & Associates, ASM International, First printing, 2000, pp. 238- 239.
12 N. A. Negm, F. M. Ghuiba and S. M. Tawfik, *Corros. Sci*., 2011, **53**, 3566.
13 H. Gräfen, E. M. Horn, H. Schlecker and H. Schindler in *"Corrosion" Ullmann's Encyclopedia of Industrial Chemistry*, Wiley-VCH: Weinheim, 2002, DOI: 10.1002/14356007.b01_08.
14 A. P. Schweitzer, in *Fundamentals of corrosion: mechanisms, causes, and preventative methods*, CRC Press, Taylor & Francis Group, 2010.
15 N. O. Obi-Egbedi and I. B. Obot, *Arabian J. Chem*., 2013, **6**, 211.
16 I. Danaee, O. Ghasemi, G. R. Rashed, M. Rashvand Avei and M. H. Maddahy, *J. Mol. Struct*., 2013, **1035**, 247.
17 P. Udhayakala, A. Jayanthi, T. V. Rajendiran and S. Gunasekaran, *Res. Chem. Intermed*., 2013, **39**, 895.
18 Z. El Adnani, M. Mcharfi, M. Sfaira, M. Benzakour, A. T. Benjelloun and M. Ebn Touhami, *Corros. Sci*., 2013, **68**, 223.
19 J. J. Fu, H. Sh. Zang, Y. Wang, S. N. Li, T. Chen, and X. D. Liu, *Ind. Eng. Chem. Res*., 2012, **51**, 6377.
20 J. J. Fu, S. N. Li, Y. Wang, X. d. Liu, L. d. Lu, *J. Mater. Sci*., 2011, **46**, 3550.
21 A. C. Tsipis, *Coord. Chem. Rev*., 2014, **272**, 1.
22 R. G. Parr and W. Yang, in *Density Functional Theory of Atoms and Molecules*, Oxford University Press, New York, 1989.
23 J. Radilla, G. E. Negrón-Silva, M. Palomar-Pardavé, M. Romero-Romo and M. Galván, *Electrochim. Acta*, 2013, **112**, 577.
24 R. G. Parr, R. A. Donnelly, M. Levy and W. E. Palke, *J. Chem. Phys*., 1978, **68**, 3801.
25 *Standard practice for conventions applicable to electrochemical measurements in corrosion testing*, ASTM G3-89, 1994.

26 A. Raman and P. Labine, in *Reviews on Corrosion Inhibitor Science and Technology*, NACE, Houston, Tex, USA, 1986.
27 M. J. Frisch, G. W. Trucks, H. B. Schlegel, G. E. Scuseria, M. A. Robb, et al., Gaussian Inc., Wallingford CT, 2004.
28 C. Pomelli, J. W. Ochterski, P. Y. Ayala, K. Morokuma, G.A. Voth, et al., Gaussian 03, Revision C.02, Pittsburgh, 2003.
29 S. G. Zhang, W. Lei, M. Z. Xia and F. Y. Wang, *J. Mol. Struct. (THEOCHEM)*, 2005, **732**, 175.
30 P. Hohenberg and W. Kohn, *Phys. Rev*., 1964, **136B**, 864.
31 A. D. Becke, *J. Chem. Phys*., 1993, **98**, 5648.
32 C. Lee, W. Yang and R. G. Parr, *Phys. Rev*., 1988, **B37**, 785.
33 *Practice for preparing, cleaning and evaluating corrosion test specimens*, ASTM G1-72, 1990.
34 O. L. J. Riggs, in *Corrosion Inhibitors*, ed. C. C. Nathan, 2nd edn., NACE, Houston, TX, 1973.
35 H. Ashassi-Sorkhabi, M. R. Majidi and K. Seyyedi, *Appl. Surf. Sci*., 2004, **225**, 176.
36 R. Solmaz, *Corros. Sci*., 2014, **81**, 75.
37 R. Solmaz, *Corros. Sci*., 2014, **79**, 169.
38 E. S. Ferreira, C. Giancomelli, F. C. Giacomelli and A. Spinelli, *Mater. Chem. Phys*., 2004, **83**, 129.
39 M. Behpour, S. M. Ghoreishi, N. Mohammadi and M. Salavati-Niasari, *Corros. Sci*., 2011, **53**, 3380.
40 R. Solmaz, E. Altunbas and G. Kardaş, *Mater. Chem. Phys*., 2011, **125**, 796.
41 I. Ahamad, C. Gupta, R. Prasad and M. A. Quraishi, *J. Appl. Electrochem.*, 2010, **40,** 2171.
42 M. Behpour, S. M. Ghoreishi, N. Mohammadi, N. Soltani and M. Salavati-Niasari, *Corros. Sci*., 2010, **52**, 4046.
43 F. B. Growcock and J. H. Jasinski, *J. Electrochem. Soc*., 1989, **136**, 2310.
44 U. Rammelt and G. Reinhard, *Electrochim. Acta*, 1990, **35**, 1045.
45 M. E. Orazem and B. Tribollet, in *Electrochemical Impedance Spectroscopy*, Wiley, Hoboken, 2008.
46 T. Tsuru, S. Haruyama and B. Gijutsu, *J. Jpn. Soc. Corros. Eng*., 1978, **27**, 573.
47 R. Solmaz, G. Kardas, B. Yazıcı and M. Erbil, *Colloids and Surfaces A: Physicochem. Eng. Aspects*, 2008, **312**, 7.
48 R. Solmaz, G. Kardas, M. Culha, B. Yazıcı and M. Erbil, *Electrochim. Acta*, 2008, **53**, 5941.
49 A. S. Baranski, P. Norouzi and J. L. Nelsson, Proc. *Electrochem. Soc*., 1996, **9**, 41.
50 M. R. Ganjali, P. Norouzi, R. Dinarvand, R. Farrokhi and A. A. Moosavi-Movahedi, *Mater Sci Eng C*, 2008, **28**, 1311.
51 P. Norouzi, B. Larijani, M. Ezoddin and M. R. Ganjali, *Mater. Sci. Eng. C*, 2009, **28**, 87.
52 P. Norouzi, B. Larijani and M. R. Ganjali, *Int. J. Electrochem. Sci*., 2012, **7**, 7313.
53 P. Norouzi, B. Larijani, M. R. Ganjali and F. Faridbod, *Int. J. Electrochem. Sci.*, 2012, **7**, 10414
54 P. Norouzi, H. Rashedi, T. M. Garakani, R. Mirshafian and M. R. Ganjali, *Int. J. Electrochem. Sci.*, 2010, **5**, 377.
55 P. Norouzi, V. K. Gupta, F. Faridbod, M. Pirali-Hamedani, B. Larijani and M. R. Ganjali, *Anal. Chem*., 2011, **83**, 1564.
56 M. Kaminski, Z. Szklarska-Smialowska, *Corros. Sci*., 1973, **13**, 557.
57 A. W. Adamson, in *A Textbook of Physical Chemistry*, Academic Press, 2nd edn., 1979.
58 E. Kowsari, M. Payami, R. Amini, B. Ramezanzadeh, M. Javanbakht, *Appl. Surf. Sci*., 2014, **289**, 478.
59 N. Soltani, M. Behpour, S.M. Ghoreishi, H. Naeimi, *Corros. Sci*., 2010, **52**, 1351.
60 R. Solmaz, M.E. Mert, G. Kardas, B. Yazici, M. Erbil, *Acta. Phys. Chem. Sin.*, 2008, **24**, 1185.
61 H. L. Wang, R. B. Liu, J. Xin, *Corros. Sci*., 2004, **46**, 2455.
62 K. Fukui, T. Yonezawa and H. Shingu, *J. Chem. Phys*., 1952, **20**, 722.
63 G. Gece, *Corros. Sci*., 2008, **50**, 2981.
64 L. Li, X. Zhang, J. Lei, J. He, Sh. Zhang and F. Pan, *Corros. Sci.*, 2012, **63**, 82.
65 *Corrosion Mechanisms*, ed. G. Trabenelli and F. Mansfeld, Marcel Dekker, NewYork, 1987.
66 A. M. Al-Sabagh, N. M. Nasser, A. A. Farag, M. A. Migahed, A. M. F. Eissa and T. Mahmoud, *Egy. J. Petro.*, 2013, 22, 101.
67 A. Zarrouk, I. El Ouali, M. Bouachrine, B. Hammouti, Y. Ramli, E. M. Essassi, I. Warad, A. Aouniti and R. Salghi, *Res. Chem. Intermed*. 2013, **39**, 1125.
68 M. J. S. Dewar and W. Thiel, *J. Am. Chem. Soc*., 1977, **99**, 4899.
69 R. G. Pearson, *Inorg. Chem*., 1988, **27**, 734.

